The nature of the red disk-like galaxies at high redshift: dust attenuation and intrinsically red stellar populations

D. Pierini,[1] C. Maraston,[2] K. D. Gordon,[3] and A. N. Witt[4] [*]

[1] *Max-Planck-Institut für extraterrestrische Physik, Giessenbachstrasse, Garching b. München, D-85748, Germany*
[2] *University of Oxford, Denys Wilkinson Building, Keble Road, Oxford, OX1 3RH, UK*
[3] *Steward Observatory, University of Arizona, Tucson, AZ 85721, USA*
[4] *Ritter Astrophysical Research Centre, The University of Toledo, Toledo, OH 43606, USA*

ABSTRACT

We investigate which conditions of dust attenuation and stellar populations allow models of dusty, continuously star-forming, bulge-less disk galaxies at $0.8 \lesssim z \lesssim 3.2$ to meet the different colour selection criteria of high-z "red" galaxies (e.g. $R_c - K > 5.3$, $I_c - K > 4$, $J - K > 2.3$). As a main novelty, we use stellar population models that include the thermally pulsating Asymptotic Giant Branch (TP-AGB) phase of stellar evolution. The star formation rate of the models declines exponentially as a function of time, the e-folding time being longer than 3 Gyr. In addition, we use calculations of radiative transfer of the stellar and scattered radiation through different dusty interstellar media in order to explore the wide parameter space of dust attenuation. We find that synthetic disks can exhibit red optical/near-infrared colours because of reddening by dust, but only if they have been forming stars for at least ~ 1 Gyr. Extremely few models barely exhibit $R_c - K > 5.3$, if the inclination $i = 90°$ and if the opacity $2 \times \tau_V \gtrsim 6$. Hence, $R_c - K$-selected galaxies at $1 \lesssim z \lesssim 2$ most probably are either systems with an old, passively evolving bulge or starbursts. Synthetic disks at $1 \lesssim z \lesssim 2$ exhibit $4 < I_c - K < 4.8$, if they are seen edge on (i.e. at $i \sim 90°$) and if $2 \times \tau_V \gtrsim 0.5$. This explains the large fraction of observed, edge-on disk-like galaxies with $K_s < 19.5$ and $F814W - K_s \gtrsim 4$. Finally, models with $2 \lesssim z \lesssim 3.2$ exhibit $2.3 < J - K < 3$, with no bias towards $i \sim 90°$ and for a large range in opacity (e.g. $2 \times \tau_V > 1$ for $i \sim 70°$). In conclusion, red disk-like galaxies at $0.8 \lesssim z \lesssim 3.2$ may not necessarily be dustier than nearby disk galaxies (with $0.5 \lesssim 2 \times \tau_V \lesssim 2$) and/or much older than ~ 1 Gyr. This result is due both to a realistic description of dust attenuation and to the emission contribution by TP-AGB stars, with ages of 0.2 to 1–2 Gyr and intrinsically red colours.

Key words: galaxies: high-redshift – galaxies: spiral – galaxies: evolution – galaxies: stellar content – dust, extinction – radiative transfer.

1 INTRODUCTION

The standard hierarchical merging scenario of structure formation and evolution (White & Rees 1978; White & Frenk 1991) is conducive to an initial formation of disks, in view of the large predicted collapse factors (Fall & Efstathiou 1980). Model stellar disks are rotationally supported and have exponential, radial surface-brightness profiles, as observed (Mo, Mao, & White 1998). A bulge+disk system forms in a two-step process: merging two equal-mass disk progenitors produces a central spheroidal component, the bulge, in the same way as an elliptical galaxy forms (see Barnes & Hernquist 1992); then gas from the surrounding dark halo cools and settles to form a new disk. Since disks of bulge+disk systems in the local Universe are a product of accretion of gas over a Hubble time, late-type spirals must form their bulges at higher redshifts than earlier types (Kauffmann 1996). In simulations of the evolution of the cosmic star-formation rate (SFR) in cold dark matter (CDM) universes, half of all stars form at $z \gtrsim 2.2$ (Hernquist & Springel 2003). Therefore, *disk galaxies* (with prolonged star-formation activity), *starburst galaxies* (with high intensity, short-lived star-formation activity), and *starbursts triggered by merging* constitute the main star factories at $z \gtrsim 2$ for hierarchical merging cosmologies.

[*] E-mail: dpierini@mpe.mpg.de, maraston@astro.ox.ac.uk, kgordon@as.arizona.edu, awitt@dusty.astro.utoledo.edu

arXiv:astro-ph/0507345v1 14 Jul 2005

Observed optical/near-infrared (IR) colours like $R - K$, or $I - K$, and $J - K$ are used to select and classify statistically high-z "red" objects. In particular, red objects at $1 \lesssim z \lesssim 2$ are expected to include systems dominated by old (i.e. with age > 1–2 Gyr), passively evolving stellar populations, with a spectral energy distribution (SED) exhibiting a well developed 4000 Å-break (rest frame), usually identified as early-type galaxies, or, conversely, dusty gas-rich systems with a continuous star-formation activity, i.e. disk galaxies (Pozzetti & Mannucci 2000). In addition, they are expected to include dusty gas-rich systems with an impulsive, very intense star-formation activity (i.e. starbursts), and the early, dusty post-starburst phases of galaxy formation that started at $1 < z < 3$ (Pierini et al. 2004a).

As a matter of fact, the observed *extremely red galaxies* (with e.g. $I - K > 4$ or $R - K > 5.3$) are very heterogeneous (Smail et al. 2002; Yan & Thompson 2003; Cimatti et al. 2003; Stevens et al. 2003; Gilbank et al. 2003; Moustakas et al. 2004; see McCarthy 2004 for a review). Morphological classifications using surface brightness profile-fitting (Cimatti et al. 2003; Gilbank et al. 2003) show that the fraction of bright (i.e. with $K < 20$) $I - K$-selected galaxies exhibiting clear disk components is about 35 ± 11 per cent. They also confirm that a further 30–37 per cent is made of spheroidal or compact systems (see Yan & Thompson 2003), while at least 15 per cent is made of disturbed or irregular objects. No link between morphological classification and spectroscopic-redshift distribution ($0.7 < z < 1.5$) exists for bright, extremely red galaxies (Cimatti et al. 2002; Yan, Thompson, & Soifer 2004).

For all these reasons, it is puzzling that extremely red optical/near-IR colours are never achieved by models of an evolving, dusty Sb-type galaxy at $z \lesssim 3$, according to Väisänen & Johansson (2004).

Interestingly, 40 per cent of the Yan & Thompson (2003) disky systems (i.e. either disk-dominated or bulge-less) with $K_s < 19.5$ and $F814W - K_s \gtrsim 4$ are viewed almost edge on (i.e. at an inclination of $\sim 90°$). Their extremely red colours are tentatively attributed to the attenuation of stellar light by dust distributed in their disks. According to Yan & Thompson, several of these edge-on disky systems possibly lie at $z < 1$, given that their large apparent sizes (several arcseconds) would lead to unusually large physical sizes (tens of kiloparsecs) for a hypothetical redshift $\gtrsim 1$. However, bright, $F814W - K_s$-selected disky galaxies do exist at $z \sim 1$ (spectroscopic, see Yan et al. 2004).

Furthermore, Labbé et al. (2003) find 6 galaxies at photometric redshifts between 1.4 and 3, with K_s-band surface brightness profiles consistent with an exponential law over 2–3 effective radii, and with face-on (i.e. viewed at an inclination of $0°$) effective radii comparable to that of the Milky Way (see also Conselice et al. 2004). All 6 large disk-like galaxies have a "red" nucleus, while their optical/near-IR colours become bluer in the outer parts. Labbé et al. (2003) can not provide a definitive interpretation of these observables, but suggest several ones: more dust, higher age, emission-line contamination, or a combination of effects, in the galaxy centres. In particular, one large disk-like galaxy at $z \sim 3$ (photometric) has $K_s = 20.53$, $F814W - K_s = 3.9$, and $J_s - K_s = 2.6$ (Förster Schreiber et al. 2004). Interestingly, Stockton, Canalizo, & Maihara (2004) have discov-

ered another disk-like galaxy at $z \sim 2.5$ (photometric) with $J - K' \sim 3.4$ and an inclination of about $70°$.

Objects with $J_s - K_s > 2.3$ are expected to be at $z > 2$, their colours being due to age and/or dust effects (Franx et al. 2003). Thus, they have been called *distant red galaxies* (van Dokkum et al. 2004). Most of the distant red galaxies studied so far exhibit red near-IR colours in the range 2.3–3.9 mag possibly as a result of a prominent Balmer break and/or 4000 Å-break moving into the J_s band, independent of their star-formation activity (Franx et al. 2003; van Dokkum et al. 2004; Förster Schreiber et al. 2004). They seem to be among the oldest (median age ~ 1–2 Gyr) and most massive (median stellar mass $\sim 10^{11}$ M$_\odot$) galaxies at $2 \lesssim z \lesssim 3.5$, with a median SFR ~ 15–150 M$_\odot$ yr^{-1} and a median rest-frame V-band attenuation $A_V \sim 0.9$–2.5 mag, according to the assumed star-formation history (Förster Schreiber et al. 2004; see also Toft et al. 2005).

However, these authors assume that the empirical "Calzetti law" for nearby starbursts (Calzetti, Kinney, & Storchi-Bergmann 1994; Calzetti et al. 2000) describes dust attenuation for any high-z, dusty stellar system. This key assumption for the SED modeling is questionable. In the local Universe, the characteristics of dust attenuation are different between starbursts, normal star-forming (i.e. non starburst) disk galaxies (Bell 2002; Gordon et al. 2004), and ultra-luminous infrared galaxies (Goldader et al. 2002). In conclusion, investigating the nature of distant, red disk-like galaxies (hereafter referred to as DRdGs, with $J - K > 2.3$) or of extremely red disk-like galaxies (hereafter referred to as ERdGs, with $I_c - K > 4$) can shed new light on the formation and evolution of disk systems.

Therefore, it is fundamental to understand if the optical/near-IR colours of DRdGs and ERdGs are due either to the luminosity-weighted age of the stellar populations present in the system or to reddening by internal dust.

To this purpose, we combine evolutionary synthesis models of stellar populations (Maraston 1998, 2005) with models of radiative transfer of the stellar and scattered radiation through the dusty interstellar medium (ISM) of a disk system (Ferrara et al. 1999; Pierini et al. 2004b).

The stellar population evolutionary synthesis models used here include the thermally pulsating Asymptotic Giant Branch (TP-AGB) phase for intermediate-mass (2–5 M$_\odot$) stars, at variance with all others (Maraston 2005). This phase is fundamental for computing correctly the SEDs of intermediate-age (i.e. between 0.2 and 1–2 Gyr) stellar populations (see Maraston 1998, 2005).

The radiative transfer models (including multiple scattering) for the disk geometry used here describe how the attenuation function[1] changes in absolute value and shape with total amount of dust and inclination of the disk, for different dust/stars configurations and different structures of the dusty ISM.

---

[1] The extinction curve describes the combined absorption and out-of-the beam scattering properties of a mixture of dust grains of given size distribution and chemical composition in a screen geometry as a function of wavelength; the attenuation function is the combination of the extinction curve with the geometry of a dusty stellar system, in which a substantial fraction of the scattered light is returned to the line of sight. We refer the reader to Calzetti (2001) for a discussion in more detail.

2 CHARACTERISTICS OF THE MODELS

2.1 Stellar populations

We assume that stellar populations are formed starting from an initial star-formation redshift z_f equal to 10. This value is between the two redshifts considered by Ciardi & Madau (2003) as markers of the epoch of reionization breakthrough in their " late reionization" and " early reionization" scenarios. We assume the so-called ΛCDM "concordance" cosmological model ($\Omega_m = 0.3$, $\Omega_\Lambda = 0.7$) with Hubble constant $H_0 = 70$ km s^{-1} Mpc^{-1}, consistent with the main *WMAP* results (Spergel et al. 2003), in order to link age (i.e. the time that has elapsed since star formation started) and redshift.

Observed red disk-like galaxies span the redshift range 0.7–3, so that we consider six representative redshifts for candidate DRdGs and ERdGs, i.e. $z = 0.83$, 1.07, 1.39, 1.85, 2.59, and 3.19, that correspond to maximum ages of the stellar populations equal to 6, 5, 4, 3, 2, and 1.5 Gyr, respectively, for $z_f = 10$. We compute additional models, where the stellar populations have a maximum age of 0.6 Gyr for any of the previous 6 redshifts, with the intent of constraining the lowest value of the parameter z_f that is necessary to reproduce the observed optical/near-IR colours of DRdGs and ERdGs.

We model the intrinsic (i.e. non attenuated by internal dust) SED of a dusty, bulge-less disk galaxy as a composite stellar population with solar metallicity ($Z_\odot$) and a Salpeter (1955) initial mass function (IMF) between 0.1 and 120 M$_\odot$. Solar metallicities seem to be present in massive, star-forming galaxies at $z \gtrsim 2$ (Shapley et al. 2004; van Dokkum et al. 2004). A "normal" IMF seems to be established when the ISM metallicity reaches a value of $\sim 10^{-4}$ Z$_\odot$ (Schneider et al. 2002). Furthermore, the Salpeter IMF describes in a consistent way different properties of the Universe at least up to $z \sim 1$ (Renzini 2004).

The intrinsic SEDs of the composite stellar populations are computed with the evolutionary synthesis code of Maraston (1998, 2005). The models include the contribution by the TP-AGB phase. TP-AGB stars are cool giants exhibiting very red optical/near-IR colours (e.g. Persson et al. 1983). They provide about 40 per cent of the bolometric luminosity and up to 80 per cent of the rest-frame K-band luminosity of an intermediate-age simple stellar population (SSP) (Maraston 1998, 2005). They are expected to play a significant role in the near-IR emission of galaxies containing 1 Gyr-old stellar populations, since the fuel consumption during the TP-AGB phase is maximum around this age (Maraston 1998, 2005). More generally, these stars must be included in any realistic modeling of stellar populations, since intermediate-mass stars do unavoidably experience the TP-AGB phase.

In the framework of this study, the effect of the TP-AGB stars will matter when the R, I, J, and K bands (i.e. those used to select high-z red galaxies) map the rest-frame near-IR. Therefore the lower redshift bins will be affected. Since the TP-AGB phase is usually not included in population synthesis models (see Maraston 2005 for examples), we have considered also some models in which the TP-AGB phase is neglected. This allows us to compare our results with others in the literature. With respect to the latter, we will show in Sect. 3.2.2 that the physically-motivated presence of TP-AGB stars softens the need either of dominant, old, passively evolving stellar populations or of large, arbitrary values of

reddening by dust associated with high SFRs to explain the observed red optical/near-IR colours of high-z galaxies.

The time dependence of the SFR[2], is described by $SFR(t) = \alpha \times e^{-\frac{t}{\tau_\star}}$ (Eq. 1), where α is the peak SFR (in M$_\odot$ yr^{-1}) and $\tau_\star$ is the SFR e-folding time, here set equal to 3, 4, 5, or 7 Gyr. We will discuss qualitatively the effects due to an alternative parameterization for the star-formation history, i.e. (e.g. Mollá, Ferrini, & Díaz 1997; Mollá, Ferrini, & Gozzi 2000) $SFR(t) = \alpha \times \frac{t}{\tau_p} e^{-\frac{t}{\tau_p}}$ (Eq. 2), where α/e represents the peak SFR, τ_p is the time when the SFR peaks, and the SFR increases linearly with time for $t < \tau_p$, but decreases exponentially with time for $t > \tau_p$[3].

Star-formation time scales as short as 3 Gyr may sound atypical, if one wants to describe properties of local, "quiescent" star-forming galaxies (see Kong et al. 2004). However, the observations seem to point to a fast evolution of disk galaxies at high z down to $z \sim 1$ (Abraham & Merrifield 2000; Kajisawa & Yamada 2001; Ravindranath et al. 2004), when the local age of the Universe was about 5.7 Gyr. Hence, a SFR e-folding time (Eq. 1) or a SFR characteristic time scale (Eq. 2) significantly shorter than 5.7 Gyr offers a simple but reasonable representation of the unknown star-formation history of a disk-like galaxy observed at $z > 1$.

The bulge-less hypothesis is explored because of the observational evidences reported in Sect. 1. In addition, we note that hints come from recent evolutionary models of star-forming, gas-rich disks (Immeli et al. 2004) that these systems may remain bulge-less for a large part of the Hubble time, if the energy dissipation of the cold cloud component is inefficient. In this case, the global SFR has a time dependence that is broadly analogous in shape to that given by Eq. 2, with a time scale longer than about 2 Gyr. We may then expect that at least disk-galaxy models with $SFR(t)$ given by Eq. 2 and τ_p set equal to 3–5 remain bulge-less within the redshift range under study. We postulate that this is so also for models where $SFR(t)$ is given by Eq. 1 with $\tau_\star \gtrsim 3$ Gyr.

---

[2] The intrinsic SEDs of the stellar population models are available at www-astro.physics.ox.ac.ik/~maraston.

[3] For reference, we give the values of the peak SFR predicted by Eq. 1 and 2 for two significant examples. The first case regards a bulge-less disk galaxy with a stellar mass of 5×10^{10} M$_\odot$ at $z = 0$ (like the Milky Way, see Dehnen & Binney 1998), that started forming stars at $z_f = 10$. The peak SFR in Eq. 1 (i.e. α) is equal to $(1-R)^{-1} \times$ 16.9, 13, 10.8, or 8.5 M$_\odot$ yr^{-1}, for $\tau_\star$ equal to 3, 4, 5, or 7 Gyr, respectively, where R is the fraction of mass in a stellar generation that is returned to the ISM over the life time of the population (Tinsley 1980). For the same end-product, if Eq. 2 holds, the peak SFR (i.e. α/e) is equal to $(1-R)^{-1} \times$ 6.6 or 5 M$_\odot$ yr^{-1} for τ_p equal to e.g. 3 or 5 Gyr, respectively. The second case is represented by a bulge-less disk galaxy with a stellar mass of 2×10^{11} M$_\odot$ at $z \sim 2.4$ (see van Dokkum et al. 2004), that started forming stars at $z_f = 10$. Now, the peak SFR in Eq. 1 is equal to $(1-R)^{-1} \times$ 1.3, 1.2, 1.1, or 1×10^2 M$_\odot$ yr^{-1}, for $\tau_\star$ equal to 3, 4, 5, or 7 Gyr, respectively. For the same end-product, the peak SFR in Eq. 2 is equal to $(1-R)^{-1} \times$ 1.5 or 2×10^2 M$_\odot$ yr^{-1} for τ_p equal to 3 or 5 Gyr, respectively.

2.2   Attenuation by internal dust

We assume that the high-z, red disk-like galaxies are axially symmetric systems, where the 3-D distribution either of stars or of dust can be parameterized by a doubly exponential law. The dust/stars configuration is preserved, whether the average disk size (for fixed luminosity) changes as a function of redshift or not (cf. Ferguson et al. 2004; Bouwens et al. 2004; Ravindranath et al. 2004)[4]. The dust/stars configuration and the properties of the dusty ISM of high-z galaxies are not well constrained by existing observations. Therefore, we adopt two different sets of Monte Carlo calculations of radiative transfer for the disk geometry, that embrace most of the parameter space defined by dust/stars configuration, structure of the dusty ISM, and dust type, that is either explored in the literature (see Bianchi 2004 for a recent review) or known from observations of normal star-forming disk galaxies in the local Universe (White, Keel, & Conselice 2000; Keel & White 2001; Dalcanton, Yoachim, & Bernstein 2004; Whittet 2003 and references therein).

The first set of simulations is taken from Pierini et al. (2004b); it illustrates results from radiative transfer models for the bulge and disk components of a late-type galaxy, based on the DIRTY code (Gordon et al. 2001). These models have been applied successfully to interpret multiwavelength photometry of edge-on late-type galaxies in the local Universe (Kuchinski et al. 1998). Here we summarize their relevant features. The radial distribution is the same for stars and dust, while the scale height of the stellar component decreases with decreasing wavelength of the stellar emission. The young stars responsible of the bulk UV emission are the most embedded in the large-scale dust distribution, that can be considered analogous to a geometrically-thin dust lane. As for the structure of the dusty ISM, this can be either homogeneous (i.e. diffuse) or two-phase, clumpy (i.e. the ISM contains diffuse gas plus molecular clouds). Dust clumps are distributed stochastically with respect to each other and to the bluest stars; the most opaque ones are located in the inner disk. The physical properties of the dust grains are assumed to be the same as those in the diffuse ISM of the Milky Way (from Witt & Gordon 2000). The opacity[5] of the disk is equal to $2 \times \tau_V$, with τ_V equal to 0.25, 0.5, 1, 2, 4, and 8. For reference, the opacity of local disks ranges between 0.5 and 2 (Kuchinski et al. 1998). Finally, only three values for the inclination i of the disk are explored here (0, 70, and 90 degrees), since reddening changes slowly with i, for $i < 70°$(e.g. Pierini et al. 2004b).

The second set of simulations is taken from Ferrara et al. (1999). There, the scale height of the stellar distribution does not depend on the wavelength of the tracing photons, and both the scale height and the scale length of the dust distribution are allowed to be larger than those of the stellar distribution. As these authors discuss, the dust-to-stars scale-height ratio has a larger effect on the attenuation

function than the dust-to-stars scale-length ratio. Therefore, we consider three dust/stars configurations, where dust and stars have the same scale length, and the dust-to-stars scale-height ratio is equal to 0.4 (corresponding to a geometrically-thin dust lane), 1, or 2.5. Ferrara et al. consider only the presence of a dusty, diffuse (or homogeneous) ISM, but with two choices for the mixture of dust grains, namely like in the Milky Way (MW) or in the Small Magellanic Cloud (SMC), as given by Gordon, Calzetti, & Witt (1997). The two dust types produce very different extinction curves at rest-frame wavelengths shorter than 2500 Å, which impacts on the observed I_c and R_c magnitudes of objects with redshift down to 2.5 and 1.7, respectively. The continuum of observed dust extinction curves is possibly caused by the environmental stresses of nearby star-formation activity (Gordon et al. 2003). Finally, we consider τ_V equal to 0.05, 0.25, 0.5, 1, 2.5, and 5, and set i equal to 9.3, 70, and 90 degrees.

Both sets of Monte Carlo computations of radiative transfer assume that the dustiest region of a disk is its centre. Hence, they consider the hypothesis that the nuclear, redder SEDs of the 6 high-z, large disk-like galaxies discovered by Labbé et al. (2003) are due to a larger dust attenuation. Conversely, these calculations do not take into account the existence of a radial gradient in the distribution of the stellar populations, a second possibility suggested by Labbé et al. as a cause for the colour gradients existing between the inner and outer regions of their sample galaxies.

2.3   Dimming due to foreground media

We do not apply corrections for dimming due either to continuum and line absorption by atomic hydrogen (HI), or to line absorption by metals, or to continuum absorption by dust, where the HI gas, metals, and dust are distributed in foreground media (clumpy or diffuse) of galactic or intergalactic nature. Hereafter we explain our reasons.

For $z \sim 3.2$ (i.e. the maximum redshift considered for our models), the HI Lyα transition at 1216 Å (rest frame) is red-shifted to ~ 5107 Å, thus shortward of the wavelength domain probed by the R_c broad-band filter. Hence, the effects of the stochastic attenuation produced by intervening HI gas (Madau 1995) do not affect at all the computation of the observed R_c magnitude and, a fortiori, of the other observed magnitudes considered in this study (see Tab. 2).

On the other hand, metal-line absorption associated with foreground systems (e.g. the damped Lyα systems, see Dessauges-Zavadsky et al. 2004) is expected to affect in a negligible way the observed optical/near-IR magnitudes and colours of galaxies at $0.8 \lesssim z \lesssim 3.2$. The cumulative effect on the optical/near-IR broad-band photometry of galaxies at these redshifts due to absorption by dust associated with individual damped Lyα systems, stochastically distributed along the line of sight, is also expected to be very small for the dust-to-gas ratios typically inferred in these systems (see Charlot & Fall 1991; Haardt & Madau 1996).

However, continuum absorption by dust distributed in the diffuse intergalactic medium (IGM) can be a source of concern especially for the observed R_c and I_c magnitudes and, thus, for the observed $R_c - K$ and $I_c - K$ colours of objects at $0.8 \lesssim z \lesssim 3.2$. In particular, this is true if the amount of IGM dust is close to the maximum value estimated by Inoue & Kamaya (2004), which is constrained by

---

[4] The exponential disk scale-length decreases with z, for $z \lesssim 1$, as $\sim (1 + z)^{-1}$ (for given rotation speed) in hierarchical models for galaxy formation (Mao, Mo, & White 1998).

[5] Hereafter, the term opacity refers to the face-on extinction optical-depth through the centre of the dusty disk at the V band. The opacity gives the total amount of dust once the dust distribution and the disk sizes are fixed (see e.g. Ferrara et al. 1999).

extinction and reddening of distant Type Ia supernovae and by the thermal history of the IGM affected by dust photoelectric heating. The physics of the ejection of dust from the ISM of a galaxy to the IGM is complex (Aguirre 1999; Bianchi & Ferrara 2005 and references therein) and opens quite different possibilities as for the IGM extinction law (see Aguirre 1999; Inoue & Kamaya 2004; Bianchi & Ferrara 2005). For instance, if only grains with sizes larger than $\sim 0.1\,\mu$m populate the IGM with an abundance large enough to account for the observed Type Ia supernova dimming at $z \sim 0.5$ (Aguirre 1999), we expect the observed $R_c - K$ and $I_c - K$ colours computed for our models with $2 \lesssim z \lesssim 3.2$ to be underestimated by up to a few tenths of a magnitude. This underestimate would be important, if true. However, the preferred interpretation for the dimming of Type Ia supernovae is the cosmological origin (see de Bernardis et al. 2000; Spergel et al. 2003). Furthermore, despite the present knowledge of the dusty IGM is poor, a dynamical model for the metal enrichment of the IGM at $z = 3$ through dust sputtering (Bianchi & Ferrara 2005) suggests that extinction and gas photoelectric heating effects due to IGM dust grains are well below current detection limits.

In conclusion, the computed R_c, I_c, J, and K magnitudes, and $R_c - K$, $I_c - K$, and $J - K$ colours reflect directly the properties assumed either for the stellar populations or for the dusty ISM of the high-z disks.

2.4 The final grid of models

Table 1 lists the characteristics of selected models of dusty, star-forming disk galaxies that will be discussed hereafter.

Column 1 shows the model index, where a different capital letter refers to the value assumed for the SFR e-folding time $\tau_\star$, and a different figure indicates either the dust/stars configuration or the structure of the dusty ISM of choice.

Column 2 shows the value assumed for $\tau_\star$ (in Gyr).

Column 3 indicates the dust/stars configuration of choice. "Standard" refers to the simulations by Pierini et al. (2004b), where the youngest stars are the most embedded in a narrow dust lane. The other acronyms refer to the simulations by Ferrara et al. (1999), where dust and stars are distributed with the same scale length but with a dust-to-stars scale-height ratio equal to 0.4 ("S01_ME04" and "S01_SE04"), 1 ("S01_ME10" and "S01_SE10"), or 2.5 ("S01_ME25" and "S01_SE25").

Column 4 indicates whether the structure of the dusty ISM is two-phase clumpy ("c") or homogeneous ("h").

Column 5 indicates whether the dust is either of MW type ("MW") or of SMC type ("SMC").

Column 6 shows the adopted radiative transfer model.

Each set of models contains 108 realizations, computed for 6 values of τ_V, 3 values of i, and 6 values of z, for a total of 3348 simulated high-z, dusty, continuously star-forming disks. We recall that the 6 redshifts correspond either to 6 different maximum ages if $z_f = 10$ (models A1 through B8), or to a fixed maximum age (i.e. 0.6 Gyr), z_f being a variable (models C1).

For these 6 redshifts, Table 2 shows how the rest-frame wavelength domain is mapped by the central wavelengths of the R_c, I_c, J, and K broad-band filters (Cousins 1978; Bessel & Brett 1988).

Table 1. Model characteristics

Den.	$\tau_\star$	dusty disk	ISM	dust type	ref.[a]
A1	5.0	standard	c	MW	1
A2	5.0	standard	h	MW	1
B1	3.0	standard	c	MW	1
B2	3.0	standard	h	MW	1
B3	3.0	S01_ME04	h	MW	2
B4	3.0	S01_ME10	h	MW	2
B5	3.0	S01_ME25	h	MW	2
B6	3.0	S01_SE04	h	SMC	2
B7	3.0	S01_SE10	h	SMC	2
B8	3.0	S01_SE25	h	SMC	2
C1	5.0	standard	c	MW	1

[a] 1: Pierini et al. (2004b); 2: Ferrara et al. (1999)

Table 2. Observed frame vs. rest frame

z	R_c	I_c	J	K
0.83	3535[a]	4298[a]	6776[a]	12076[a]
1.07	3125	3799	5904	10676
1.39	2707	3291	5188	9247
1.85	2270	2760	4351	7754
2.59	1802	2191	3454	6156
3.18	1548	1881	2966	5287

[a] the rest-frame wavelength (in Å) mapped by the central wavelength of each broad-band filter as a function of z

3 RESULTS

3.1 Effects due to dust attenuation

In this section we focus on the parameters describing the attenuation by internal dust (see Sect. 2.2), an aspect neglected by studies of high-z galaxies that make use of the Calzetti law in a blind way.

Here we anticipate that the characteristics of dust attenuation affect more the R_c magnitude than the K magnitude, and turn out to be more sensitive parameters at higher redshifts, since dust absorbs and scatters more at rest-frame UV–optical wavelengths than at rest-frame near-IR ones, whatever its type (e.g. Whittet 2003).

3.1.1 Effects due to structure of the dusty ISM, opacity, or inclination

Figure 1 shows how the observed R_c and K magnitudes depend on the structure (two-phase clumpy vs. homogeneous) assumed for the dusty ISM, as a function of opacity, inclination, and redshift. This is illustrated through models B1 and B2, both with $\tau_\star = 3$ Gyr, where the youngest stars are the most embedded in a narrow dust lane.

A homogeneous dusty ISM is more "opaque" than a two-phase clumpy one (e.g. Witt & Gordon 1996, 2000). However, the size of the relative absorption/scattering efficiency between the two structures of a dusty ISM depends on opacity and inclination of the disk, as quantified by Pierini et al. (2004b). In fact, for the disk geometry, it is the total attenuation along the observer's line of sight what counts. In general, a face-on disk becomes more opaque at a given rest-

frame wavelength when the total amount of dust (i.e. the opacity) increases; this is even more so if dust is distributed in a diffuse ISM. Conversely, an edge-on disk becomes soon very opaque when the opacity increases, so that differences in the structure of its dusty ISM become unimportant.

For reference, Fig. 1 shows also the effect of increasing the SFR e-folding time to 5 Gyr (i.e. models A1 vs. B1). At lower redshifts (i.e. $z \lesssim 1.4$) the observed optical/near-IR magnitudes are more sensitive to the star-formation history than to the structure of the dusty ISM. The opposite is true for $z > 1.4$, especially if the disk model has a large opacity (i.e. $2 \times \tau_V > 2$) and is viewed at $i \lesssim 70°$. In general, as redshift decreases, star-formation effects are larger on the R_c magnitude than on the K magnitude, simply because the R_c band probes the light from the youngest stars.

3.1.2   Effects due to dust/stars configuration or dust type

Figures 2 and 3 illustrate the sensitivity of the models to dust/stars configuration and dust type, for a fixed SFR e-folding time (i.e. 3 Gyr) and for a dusty diffuse ISM (i.e. for models B3 through B8 in Tab. 1). We recall that stars become more embedded in the dusty disk when the dust/stars configuration changes from S01_ME04 (or S01_SE04) to S01_ME25 (or S01_SE25). In general, stellar light is attenuated and reddened more efficiently when the dust-to-stars scale-height ratio increases from 0.4 to 2.5 (Ferrara et al. 1999). Therefore, the kind of extinction law becomes more important when the dust-to-stars scale-height ratio of the model increases, opacity and inclination being fixed.

Differences in the observed R_c or K magnitude due to a change in the dust/stars configuration increase (in absolute value) when either the opacity or the inclination of the model increases, whatever the dust type (see Fig. 2 for MW-type dust). Interestingly, inclination effects are not negligible and may not follow intuition. For instance, an edge-on disk at high z has a brighter R_c magnitude when its stellar populations are fully embedded in the dusty ISM (i.e. for the dust/stars configuration S01_ME25 or S01_SE25), if $2 \times \tau_V < 2$.

The explanation of this apparent paradox is the following. For an edge-on disk with $2 \times \tau_V < 2$, the dust column density along the line of sight, averaged over the projection of the stellar disk onto the sky plane, is lower the larger the dust-to-stars scale-height ratio. In addition, scattering on dust grains is directed forward at the rest-frame UV–blue wavelengths probed by the R_c band; hence, more scattered UV–blue photons will leave the edge-on disk at high z when $2 \times \tau_V < 2$. Conversely, for an edge-on disk with $2 \times \tau_V >> 2$, the blocking action of the dusty ISM increases across a larger region of the dusty disk overlapping with the stellar disk the larger the dust-to-stars scale-height ratio. A similar explanation applies to the behaviour of the observed K magnitude. Dust grains not only absorb less but also scatter less and at a wide angle at the rest-frame visual–near-IR wavelengths probed by the K band. Hence, for an edge-on disk with $2 \times \tau_V < 2$, more (rest-frame) visual–near-IR photons will be returned to the observer's line of sight, traveling through the dusty disk along different directions initially, the larger the dust-to-stars scale-height ratio.

Figure 3 shows that a change in the extinction law has a relevant impact on the R_c magnitude when the R_c band
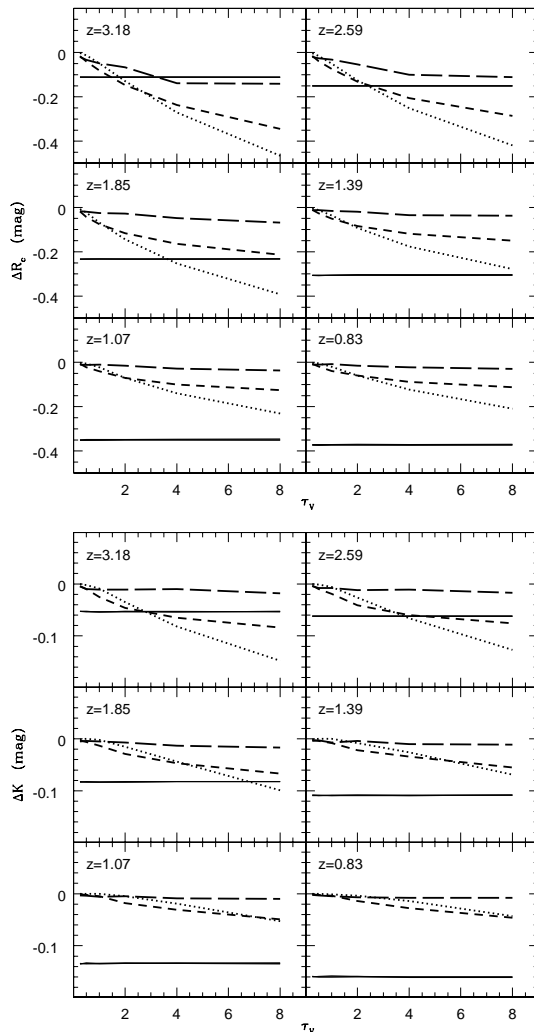
Figure 1. The difference (Δ) either in R_c magnitude (top) or in K magnitude (bottom) produced by a two-phase clumpy structure of the dusty ISM with respect to a homogeneous one (i.e. models B1 vs. B2) is plotted as a function of opacity ($2 \times \tau_V$), inclination (i), and redshift (z). Dotted, short-dashed, and long-dashed lines connect models with $i = 0°$, $70°$, and $90°$, respectively. Models B1 and B2 assume the youngest stars to be the most embedded in a narrow dust lane, and $\tau_\star = 3$ Gyr. Solid lines show the magnitude differences when $\tau_\star$ increases to 5 Gyr (i.e. models A1 vs. B1).

maps rest-frame UV wavelengths. For instance, for $z \sim 3.2$, SMC-type dust produces a fainter R_c magnitude with respect to MW-type dust, the relative dimming being of 0.6–0.8 mag at maximum, as a function of inclination, for the models with dust-to-stars scale-height ratio equal to 2.5 and $\tau_\star = 3$ Gyr reproduced there. This differential effect is reduced for $z \sim 1.85$, when the red-shifted 2175 Å-absorption feature of MW-type dust falls inside the R_c band; it amounts up to 0.3 mag for lower redshifts of the models. SMC-type dust produces also a slightly fainter K magnitude, by 0.25 mag at maximum, with respect to MW-type dust. In conclusion, studies aimed at unraveling the extinction curves of high-z objects are urged (e.g. Hirashita et al. 2005).
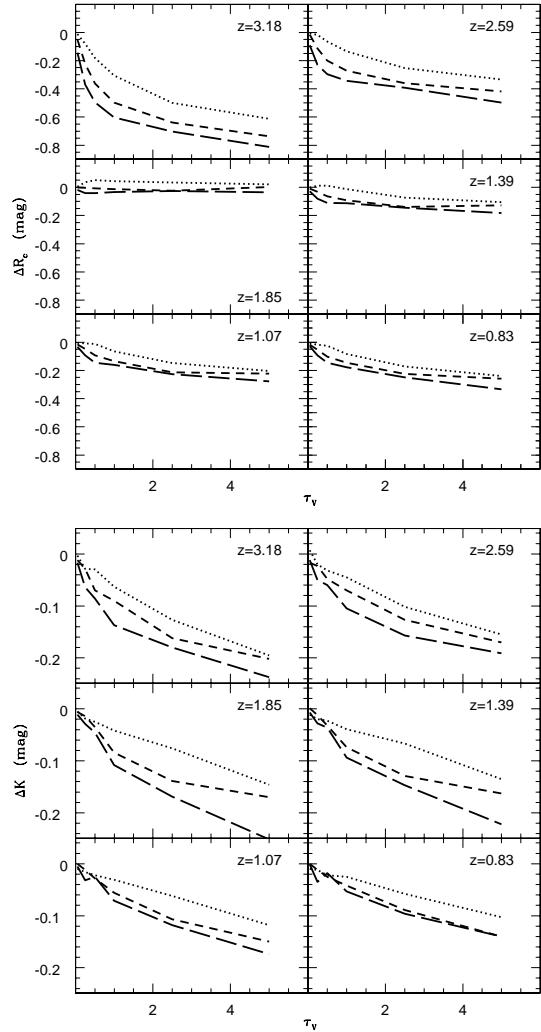
As it can be inferred from Fig. 3, a change in the extinc-
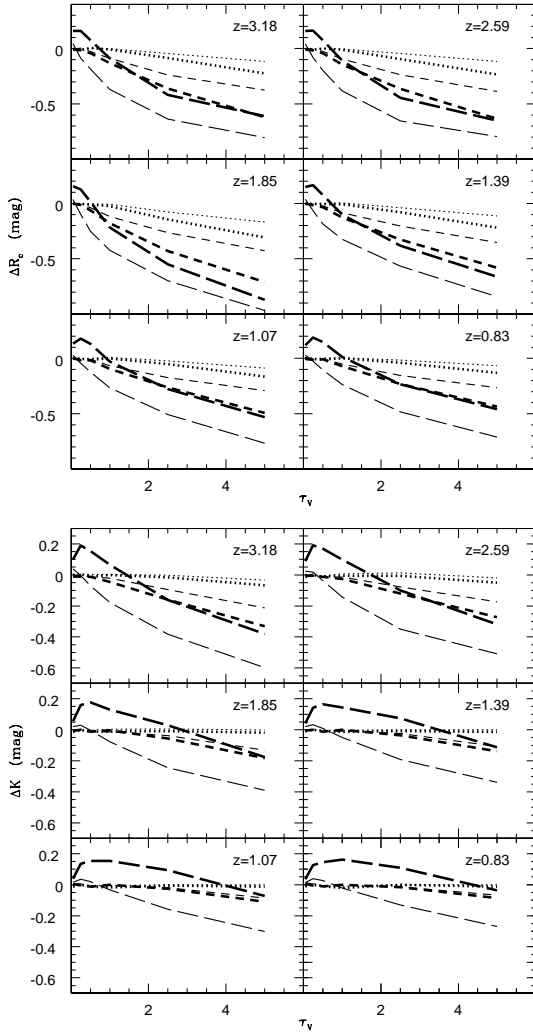
Figure 2. The difference either in R_c magnitude (top) or in K magnitude (bottom) between models B3 and B4 (thin lines) or models B3 and B5 (very thick lines) is plotted as a function of opacity, inclination, and redshift. Dotted, short-dashed, and long-dashed lines connect models with $i = 9.3°$, $70°$, and $90°$, respectively. Models B3, B4, and B5 assume $\tau_\star = 3$ Gyr, a diffuse ISM with MW-type dust, and a dust-to-stars scale-height ratio equal to 0.4, 1, and 2.5, respectively.

Figure 3. The difference either in R_c magnitude (top) or in K magnitude (bottom) produced by the MW extinction law with respect to the SMC one (i.e. models B5 vs. B8) is plotted as a function of opacity, inclination, and redshift. Dotted, short-dashed, and long-dashed lines connect models as in Fig. 2. Models B5 and B8 assume $\tau_\star = 3$ Gyr, a dusty, diffuse ISM, and a dust-to-stars scale-height ratio equal to 2.5.

tion law produces a remarkable difference (up to 0.6 mag) in the observed optical/near-IR colours of the models only when the R_c and I_c broad-band filters map the rest-frame spectral region around 2175 Å. This happens for redshifts around ~ 2 and ~ 3 for the R_c and I_c filters, respectively.

3.2   Models vs. observations

### 3.2.1   When high-z, dusty star-forming disks are "red"

The results illustrated in Sect. 3.1.1 and 3.1.2 demonstrate that the interpretation of the SEDs of high-z galaxies depends in a very sensitive way on the assumptions made for describing dust attenuation. Once a realistic description of dust attenuation in non-starburst (disk) galaxies is adopted,

do synthetic, high-z, dusty star-forming disks exhibit the red colours identifying real DRdGs and ERdGs? Hereafter we discuss which models are selected as DRdGs and/or ERdGs. In particular, Fig. 4 and 5 illustrate results for models with extreme properties as for the dust/stars configuration and the extinction law (models B1, B5, and B8).

As a first main result, we find that the synthetic, dusty star-forming disks that meet the colour selection criterion for distant red galaxies (i.e. $J - K > 2.3$) are mostly at $2 \lesssim z \lesssim 3.2$, consistent with Franx et al. (2003); no model at $z < 1$ exhibits $J - K > 2.3$. Models at $2 \lesssim z \lesssim 3.2$ can exhibit values of $J - K$ as red as 3 mag at maximum, as it can be inferred from Fig. 4 and 5, and from the considerations in Sect. 3.1.1 and 3.1.2. Hence, they can account for a large fraction of the $J_s - K_s$ colours of the 34 real, distant red galaxies at (photometric) redshift between 2 and
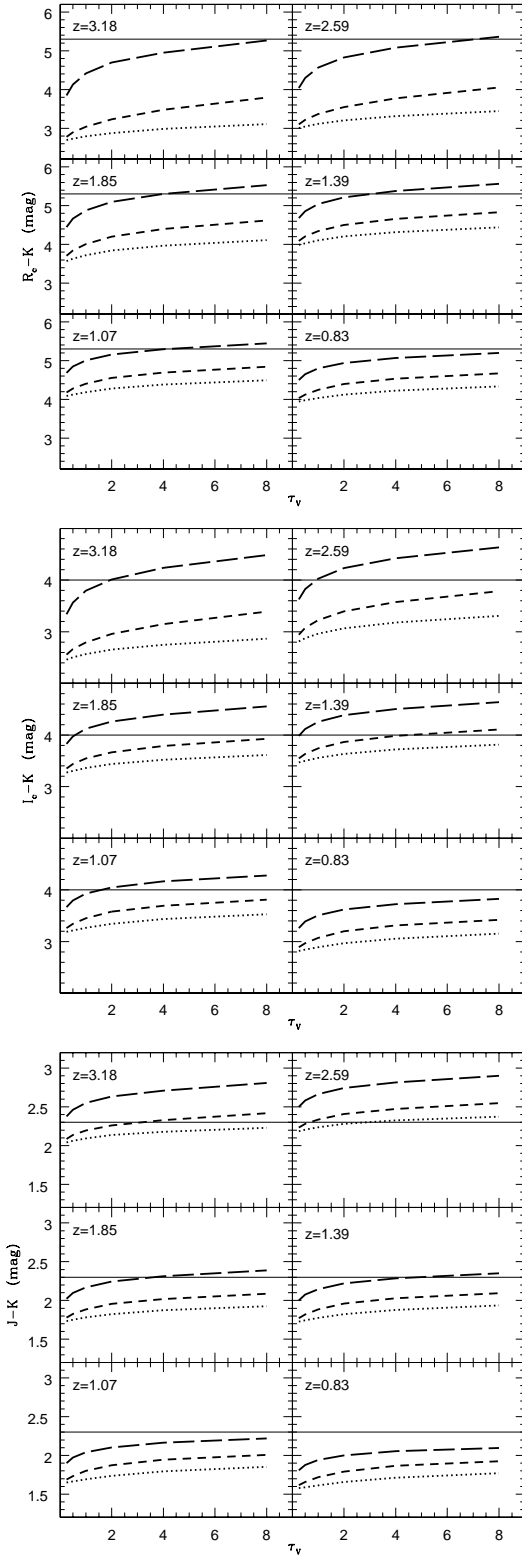
Figure 4. $R_c - K$ (top), $I_c - K$ (middle), and $J - K$ (bottom) are shown as a function of τ_V, i, and z for models B1, where the youngest stars are the most embedded in a narrow lane with MW-type dust and a two-phase clumpy structure, and $\tau_\star$ is equal to 3 Gyr. Dotted, short-dashed, and long-dashed lines connect models with $i = 0°$, $70°$, and $90°$, respectively. Horizontal, solid lines show the different colour-selection criteria for high-z red galaxies.
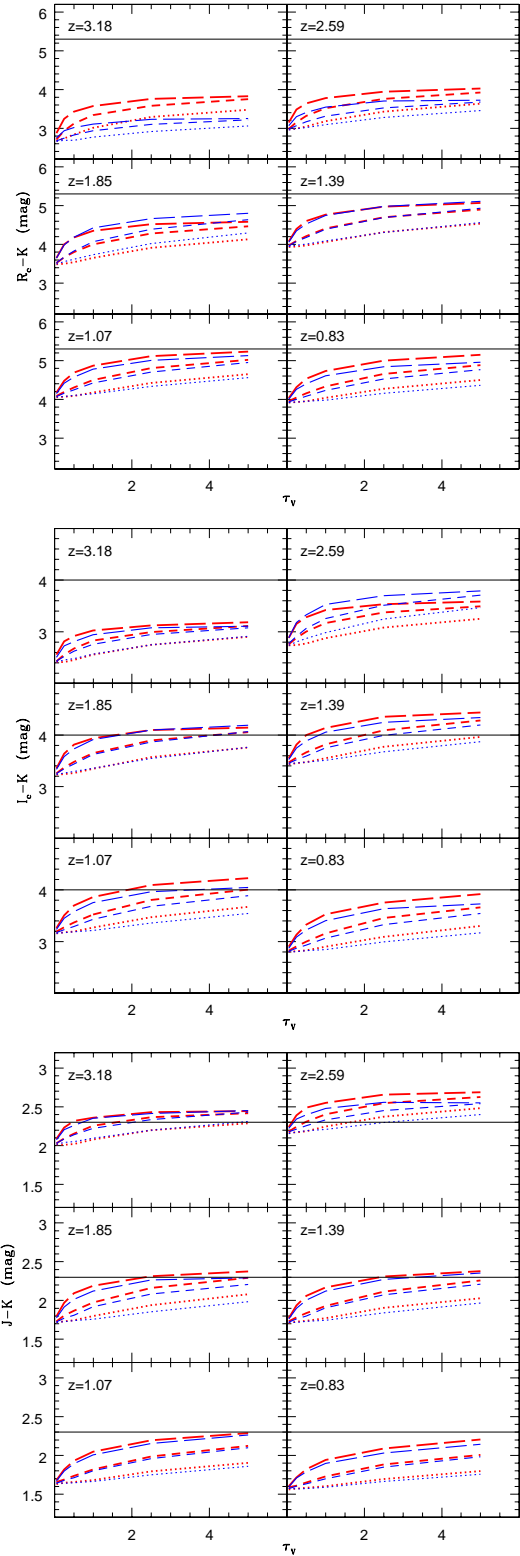
Figure 5. The same as in Fig. 4 but for models B5 (blue/thin lines) and B8 (red/thick lines), where $\tau_\star$ is equal to 3 Gyr, the dusty ISM is diffuse, the dust-to-stars scale-height ratio is equal to 2.5, but dust is either of MW-type or of SMC-type, respectively. Dotted, short-dashed, and long-dashed lines connect models with $i = 9.3°$, $70°$, and $90°$, respectively. Horizontal, solid lines are the same as in Fig. 4.

3.5 investigated by Förster Schreiber et al. (2004). In fact, for this sample, the median, mean, and rms values of $J_s - K_s$ are equal to 2.7, 2.8, and 0.43 mag, respectively.

However, our models can not reproduce $J_s - K_s$ colours in the range 3–3.9 mag, as observed for 12 of these 34 distant red galaxies. Objects with $J - K \gtrsim$ 3–4 were already observed by Maihara et al. (2001). These "hyper extremely red objects" have been proposed to be primordial elliptical galaxies reddened by dust and still in the starburst phase of their formation at $z \sim 3$ and, thus, to be the counterparts of the brightest sub-mm sources (Totani et al. 2001). However, a bulge+disk galaxy can offer a viable alternative to the interpretation as starbursts of some of the previous 12 distant red galaxies at $2 \lesssim z \lesssim 3.5$ with $3 < J_s - K_s < 3.9$, especially when considering that the properties of dust attenuation are different between the bulge and disk components (e.g. Pierini et al. 2004b).

In addition, we find that most of the $J - K$-selected models have $i \sim 90°$, despite the very different dust/stars configurations, structures of the dusty ISM, and kinds of extinction law explored here. The opacity of the $J - K$-selected edge-on models at $2 \lesssim z \lesssim 3.2$ can be much less than 0.5. On the other hand, a few $J - K$-selected edge-on models have redshifts as low as 1.4 if they are very opaque (e.g. $2 \times \tau_V \gtrsim 8$ for models B1 in Fig. 4 or $2 \times \tau_V \gtrsim 6$ for models B8 in Fig. 5). However, synthetic $J - K$-selected disks at $2 \lesssim z \lesssim 3.2$ can be viewed at inclinations as low as 0 degrees, if their opacity is large enough (e.g. $2 \times \tau_V \gtrsim 6$ for models B1 in Fig. 4 or $2 \times \tau_V > 4$ for models B8 in Fig. 5).

Unfortunately, there is almost no morphological information for the Förster Schreiber et al. (2004) sample at the moment of writing, except for the DRdG discovered by Labbé et al. (2003), exhibiting $J_s - K_s = 2.6$ and $F814W - K_s = 3.9$. In order to reproduce the optical/near-IR colours of this large disk-like galaxy at $z = 2.94$ (photometric), seemingly viewed at $i < 70°$, with e.g. a dust/stars configuration like that of Pierini et al. (2004a), one has to invoke $\tau_\star < 3$ Gyr. Hence, this object might be either experiencing or on the verge of a central gas+stars instability (see Immeli et al. 2004). Similar conclusions may apply to the disk-like galaxy at $z \sim 2.5$ (photometric) with $J - K' \sim 3.4$ and $i \sim 70°$ discovered by Stockton et al. (2004).

Interestingly, Toft et al. (2005) conclude that the rest-frame UV and optical surface brightness distributions of their 5 $J - K_s$-selected galaxies at $z \gtrsim 2$ (photometric) are better represented by exponential disks than by $r^{1/4}$ laws. Two of these disk galaxies (at $z = 2.2$ and 1.9) certainly host active galactic nuclei (AGN, see also Rubin et al. 2004) and, thus, have bulges, if the link beetwen super massive black holes and bulges found in the local Universe holds at high redshifts (Page et al. 2004). Their $J - K_s$ colours (2.42 and 2.66 mag) are not particularly red however: the high-inclination disk-like galaxy at $z = 1.8$ of Toft et al. (2005) exhibits $J - K_s = 2.45$.

In conclusion, our $J - K$-selected models of dusty, star-forming, bulge-less disk galaxies do not necessarily suffer from large rest-frame V-band attenuations. This conclusion holds even though a decrease of τ_V by a factor of about 2 can be produced by an equivalent decrease of $\tau_\star$, all the other model parameters being fixed (not shown). It also holds whatever the dust/stars configuration, the structure

of the dusty ISM, or the dust type, for fixed star-formation history[6].

This result is at variance with that of Förster Schreiber et al. (2004), in case most of their observed distant red galaxies are indeed bulge-less disk galaxies at $2 \lesssim z \lesssim 3.5$. For instance, 2 Gyr-old (at $z = 2.59$) models B1 with $\tau_\star = 3$ Gyr exhibit $2.3 < J - K < 2.5$ already for $i \sim 70°$, if $2 \times \tau_V > 1$, i.e. for a rest-frame V-band attenuation along the line of sight larger than ~ 0.2 mag, and $2.3 < J - K < 2.4$ for $i \sim 0°$, if $2 \times \tau_V \gtrsim 6$, i.e. for a rest-frame V-band attenuation along the line of sight larger than ~ 0.3 mag (see Fig. 4). Conversely, the model-fitting technique adopted by Förster Schreiber et al. gives median ages equal to 1 or 2 Gyr and, respectively, median values of A_V equal to 0.9 or 2.5 mag when the SFR is assumed either to decline exponentially with time as in Eq. 1 but with $\tau_\star = 0.3$ Gyr or to be constant.

The discrepant conclusions can be explained as follows. Firstly, a realistic description of dust attenuation for the disk geometry (but not only, see e.g. Witt & Gordon 2000), as from radiative transfer calculations, shows that the ratio of UV-to-visual attenuation changes significantly and non monotonically as a function of the V-band attenuation (e.g. Ferrara et al. 1999; Tuffs et al. 2004; Pierini et al. 2004b). Conversely, this ratio is "frozen" in the Calzetti law adopted by Förster Schreiber et al. (2004), as shown by e.g Pierini et al. (2004a, their fig. 2).

Secondly, the TP-AGB phase included in the stellar population models impacts on their rest-frame visual–near-IR SEDs (see Maraston 2005) in a way that produces intrinsically redder, observed near-IR colours for $2 \lesssim z < 3.2$. Förster Schreiber et al. (2004) resort to the Bruzual & Charlot (2003) stellar population evolutionary synthesis models that do not include the TP-AGB phase (see Maraston 2005). We have evaluated the reddening produced by the TP-AGB phase (up to ~ 0.2 mag in the observed $J - K$ and $I_c - K$, and up to ~ 0.3 mag in the observed $R_c - K$) by computing equivalent models in which the TP-AGB phase was neglected on purpose. The effect of the TP-AGB phase depends obviously on the redshift, because it is necessary that the observed frame probes the near-IR rest-frame where the TP-AGB stars emit most of their energy (see Sect. 2.1). Moreover, the ratio between the numbers of old and intermediate-age stars increases together with the age (i.e. with decreasing redshift). As a consequence, the impact of the emission from TP-AGB stars on the composite stellar population models considered here is maximum for $1 \lesssim z \lesssim 2$, when the age of the models approaches the SFR e-folding time.

In conclusion, the effect of TP-AGB stars is to allow more models of dusty, star-forming disks at $0.8 \lesssim z \lesssim 3.2$ to be selected as either DRdGs or ERdGs, and to reduce the needed amount of dust by up to a factor of two (see Fig. 6).

As for ERdGs, the $I_c - K$-selected models at $1 \lesssim z \lesssim 2$ need to have an inclination of 90°, but in case the dusty ISM is diffuse and the dust-to-stars scale-height ratio is equal to 2.5, $i \sim 70°$ is sufficient (see Fig. 5). The synthetic, $I_c - K$-selected edge-on disks exhibit a large range in opacity (i.e.

---

[6] The simultaneous presence of SMC-type dust and of a geometrically-thin dust lane where the youngest stars are the most embedded maximizes the fraction of successful models.

$2 \times \tau_V \gtrsim 0.5$), according to the dust/stars configuration, the structure of the dusty ISM, the dust type, and the star-formation history. The value of the rest-frame V-band attenuation of the $I_c - K$-selected edge-on models is very sensitive to all these parameters. For instance, edge-on models A1 at $z = 1.39$ exhibit $4 < I_c - K \lesssim 4.5$ for $2 \times \tau_V > 1$, i.e. for values of the rest-frame V-band attenuation along the line of sight larger than ~ 0.8 mag. Reducing $\tau_\star$ from 5 to 3 Gyr makes the edge-on models B1 at $z = 1.39$ span a similar colour range ($4 < I_c - K \lesssim 4.6$) but already for $2 \times \tau_V > 0.5$, i.e. for values of the rest-frame V-band attenuation along the line of sight larger than 0.5 mag. Conversely, edge-on models B3 and B6, with a dust-to-stars scale-height ratio equal to 0.4, never exhibit $I_c - K > 4$. We conclude that real $I_c - K$-selected, edge-on disk-like galaxies at $1 \lesssim z \lesssim 2$ are not necessarily more opaque, and, thus, dustier than nearby disk galaxies, for which $0.5 \lesssim 2 \times \tau_V \lesssim 2$ (Kuchinski et al. 1998).

Far-IR photometry of high-z red disk-like galaxies with *Spitzer* and *Herschel* will offer a decisive test for this conclusion. This holds for DRdGs at $2 \lesssim z \lesssim 3.2$ as well.

The previous result is new and encouraging for the following reasons. Firstly, the unspecified model SEDs for Sb-type galaxies adopted by Väisänen & Johansson (2004) from the GRASIL model library (Silva et al. 1998) failed to reproduce the optical/near-IR colours identifying extremely red galaxies, that do contain late-type galaxies (Yan & Thompson 2003; Cimatti et al. 2003; Gilbank et al. 2003). This is most probably due to the use of angle averaged, standard GRASIL models for Sb galaxies, where dust and stars have the same spatial distribution (see Silva et al. 1998).

Secondly, and most importantly, HST imaging in the F814W broad-band filter of $F814W - K_s$-selected galaxies with $K_s < 19.5$ shows that one third of this sample is made of disky systems (i.e. disk-dominated or bulge-less) viewed almost edge on (Yan & Thompson 2003). Moreover, a few edge-on ERdGs exhibit narrow dust lanes beyond any doubt, thanks to the superb spatial resolution of HST. Now, Yan & Thompson conclude that most of their edge-on disky systems lie possibly at $z < 1$, otherwise these systems would be too large. However, bright, $F814W - K_s$-selected disk-like galaxies do exist at $z \sim 1$ (Yan et al. 2004) and our models can explain this finding.

At this point we note that 3 out of the 7 $F814W - K_s$-selected, disk-dominated galaxies with spectroscopic redshifts around 1 and classified as absorption-line objects by Yan et al. (2004) are viewed close to edge on, and 6 out of the 13 objects without measured redshifts are also disk-dominated galaxies seen edge on. Yan et al. suggest that the absence of detected spectral features (in the observed range 5500–9000 Å) may be due to their weakness, owing to dust attenuation (emission lines) and/or to the intrinsic mixture of stellar populations (emission and absorption lines). Our result confirms that weak spectral features may be due to an increased contribution of intermediate-age stellar populations to the total bolometric luminosity of the ensamble of stars present in the previous $F814W - K_s$-selected disk-dominated galaxies, without invoking extremely large amounts of dust.

Finally, only a handful models can meet the $R_c - K > 5.3$ colour-selection criterion for extremely red galaxies at $1 \lesssim z \lesssim 2$. They all have a geometrically-thin dust lane
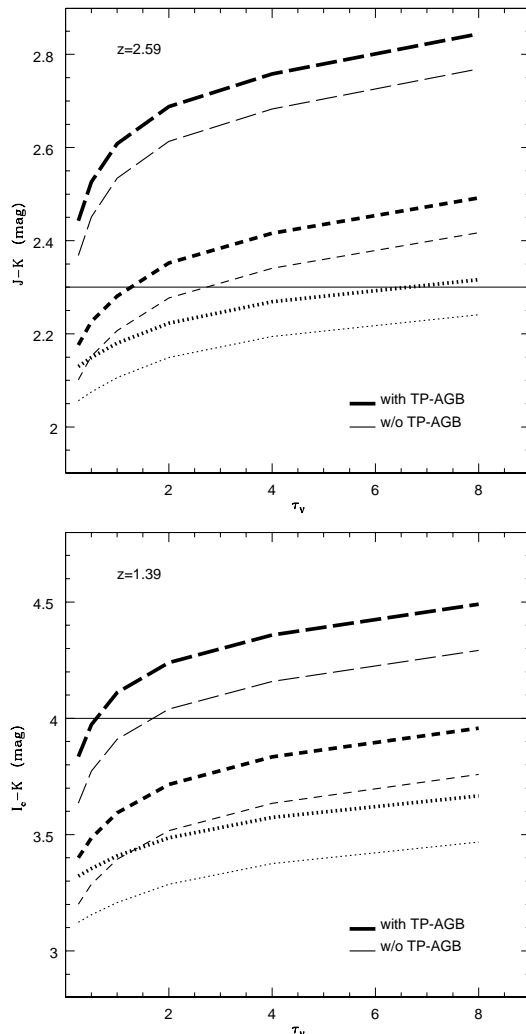
Figure 6. $J - K$ (top) and $I_c - K$ (bottom) are plotted as a function of τ_V and i for models A1 at, respectively, $z = 2.59$ and $z = 1.39$ (thick lines) and for equivalent models in which the TP-AGB phase was neglected on purpose (thin lines). Dotted, short-dashed, and long-dashed lines connect models with $i = 0°$, $70°$, and $90°$, respectively. Horizontal, solid lines show the appropriate colour-selection criterion.

where the youngest stars are the most embedded in, a very large opacity (i.e. $2 \times \tau_V \gtrsim 8$), and an inclination of $90°$. No unambiguous discovery of $R_c - K$-selected, bulge-less disk galaxies at redshifts between 1 and 2 is reported in the literature (see e.g. Sawicki et al. 2005). The absence of continuously star-forming, bulge-less disk galaxies at $1 \lesssim z \lesssim 2$ in $R_c - K$-selected samples is due to a selection effect, the $R_c - K > 5.3$ threshold being too red for such objects (as explained in Sect. 3.2.8).

3.2.2   On the epoch of initial star formation

Figure 7 shows the distribution in the $R_c - K$ vs. $J - K$ and $I_c - K$ vs. $J - K$ colour–colour plots of models A1, with ages between 1.5 and 6 Gyr for z between 3.2 and 0.8, respectively, and for 0.6 Gyr-old models of dusty star-forming

disks at $0.8 \lesssim z \lesssim 3.2$ (models C1). For these two sets of models with $\tau_\star = 5$ Gyr, the dust/stars configuration, the local dust distribution, and the dust type are the same.

In order to reproduce red near-IR colours (i.e. $J - K > 2.3$) or extremely red optical/near-IR colours (i.e. $I_c - K > 4$), the time that has elapsed since star formation started is at least ~ 1 Gyr at the redshift of the colour-selected model. Otherwise, either dust attenuation for the high-z objects is not described as for disk galaxies in the local Universe, or bulge-less disk galaxies with star-formation time-scales of the order of ~ 1 Gyr do exist at high z.

Comfortably, evolved stellar populations seem to be present in bright, $F814W - K_s$-selected, edge-on disk-dominated galaxies classified as absorption-line systems (Yan et al. 2004).

On the other hand, also Förster Schreiber et al. (2004) conclude that the median time that has elapsed since star formation started ranges between 1 and 2 Gyr for their sample of $J - K$-selected galaxies at $2 \lesssim z \lesssim 3.5$ (photometric). Therefore, our conclusion on the formation epoch of DRdGs at these redshifts is consistent with that of Förster Schreiber et al., though we fear that the assumptions behind their models may lead to an artificial increase of the ages and/or the values of the rest-frame V-band attenuation given by their best-fit solutions in case of disks (see Sect. 3.2.1). The same applies to the model-fitting results of Toft et al. (2005).

3.2.3 The co-moving space density of high-z red disk-like galaxies

Here we discuss the observability of the models. Figure 8 reproduces the $I_c - K$–K and $J - K$–K colour–magnitude diagrams for models A1. In addition, for $z \leqslant 2.59$, it reproduces analogous models in which the TP-AGB phase was neglected on purpose, in order to visualize the effect of the neglection of this phase. In fact, at those redshifts, the observed-frame near-IR broad-band filters sample a portion of the intrinsic spectrum that is affected by the TP-AGB phase. The total stellar mass of all models is set equal to 10^{11} M$_\odot$ whatever z. Note that the observed K luminosity at redshifts ~ 1 would be 25 per cent fainter if the TP-AGB phase had not been included.

Now, assuming that models A1 picture fairly well real dusty, continuously star-forming disk-like galaxies observed at high z, what should one expect for the co-moving space density of real DRdGs and ERdGs?

As Fig. 8 shows, models A1 with $J - K > 2.3$ and a stellar mass of 10^{11} M$_\odot$ at $2 \lesssim z \lesssim 3.2$ meet the faintest detection limit of present deep K-band surveys (i.e. ~ 22.5 K-mag). In particular, a few of them do so already for a K-band limit of 21 mag, for $z \sim 2.6$. From Fig. 8, it is straightforward to conclude that synthetic, dusty star-forming disks like models A1 can be detected down to 22.5 K-mag if they are more massive than $\sim 10^{10}$ M$_\odot$. Hence, if massive, bulgeless disk galaxies exist at high z, and if they have properties like our models, then they contribute up to 70 per cent (cf. Sect. 3.2.1) of the estimated surface density of distant red galaxies (3 ± 0.8 arcmin^{-2}, see Franx et al. 2003). Furthermore, a noticeable field-to-field variation may be expected in their counts if they are selected owing to inclination effects. Förster Schreiber et al. (2004) report field-to-field variations (by a factor of 2 on average) of the surface density
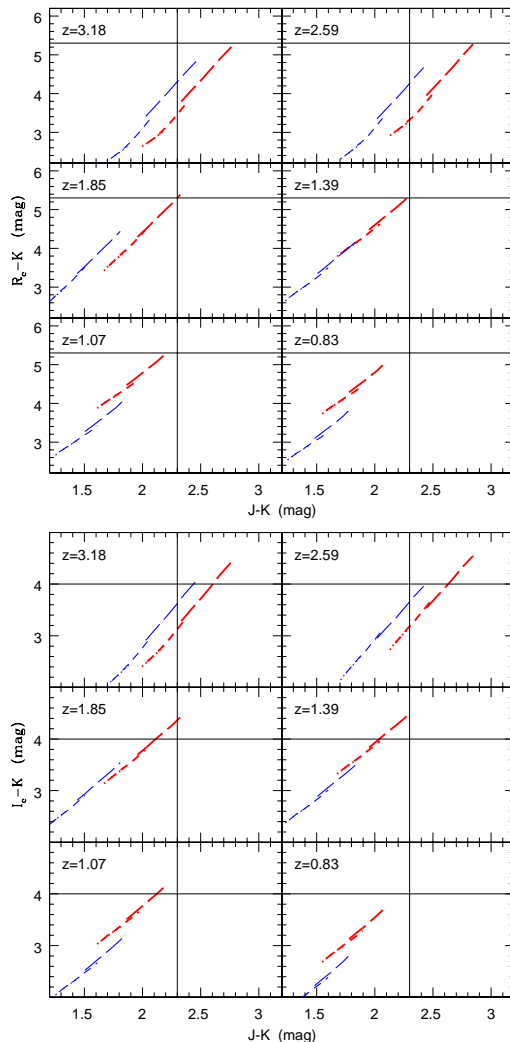
Figure 7. $R_c - K$ vs. $J - K$ (top) and $I_c - K$ vs. $J - K$ (bottom) are shown as a function of opacity, inclination, and redshift for models C1 (blue/thin lines) and A1 (red/thick lines), where the youngest stars are the most embedded in a narrow lane with MW-type dust and a two-phase clumpy structure, and $\tau_\star = 5$ Gyr. However, models C1 are 0.6 Gyr old whatever z, while models A1 age with decreasing redshift, having $z_f = 10$. Dotted, short-dashed, and long-dashed lines connect models with $i = 0°$, $70°$, and $90°$, respectively; for each line, the opacity of the model increases from bottom left to top right. In each panel, horizontal and vertical, black solid lines show the colour selection criteria for extremely red galaxies and distant red galaxies, respectively.

of their $J - K$-selected galaxies. However, a complete morphological information is not available for these galaxies. Förster Schreiber et al. note that cosmic variance could easily account for a large part of the differences in the surface densities. Conversely, if real DRdGs at $2 \lesssim z \lesssim 3.5$ are less massive than 10^{10} M$_\odot$ (stellar mass), and if they have properties like our models, then they would escape detection even in the present, deepest K-band surveys. In this case, their co-moving space-density can not be constrained by present observations.

On the other hand, edge-on, dusty, continuously star-
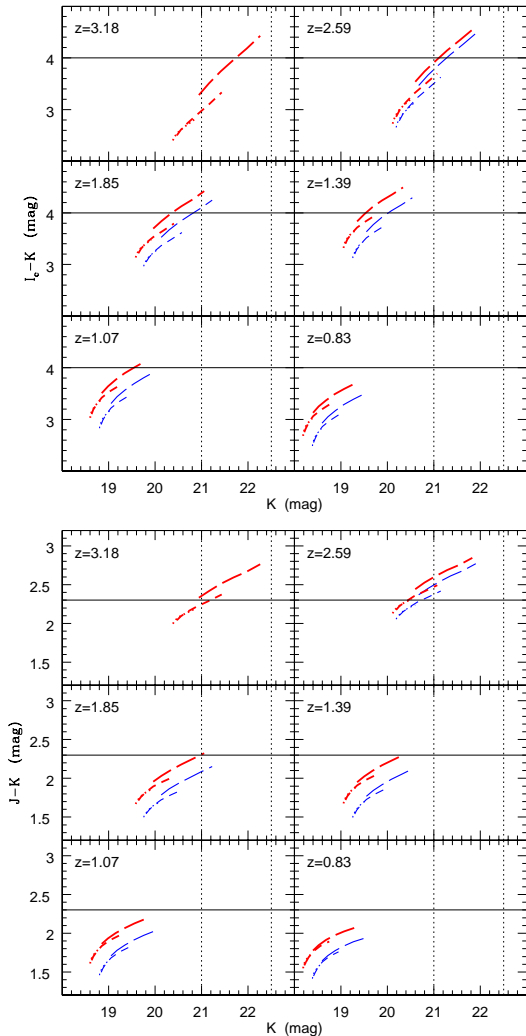
Figure 8. $I_c - K$ (top) and $J - K$ (bottom) vs. K magnitude are shown as a function of opacity, inclination, and redshift for models A1 (red/thick lines) as an observability check. For $z \leqslant 2.59$, these colour–magnitude diagrams contain also equivalent models in which the TP-AGB phase was neglected on purpose (blue/thin lines) in order to visualize the effect of the neglection of this phase. The stellar mass of all models is set equal to 10^{11} M$_\odot$ whatever z. Dotted, short-dashed, and long-dashed lines connect models with $i = 0°$, $70°$, and $90°$, respectively; for each line, the opacity of the model increases from bottom left to top right. In each panel, the horizontal, black solid line shows the appropriate colour-selection criterion, while the two vertical, black dotted lines show typical limits of present, deep K-band surveys.

forming disk-like galaxies at $1 \lesssim z \lesssim 2$ with $I_c - K > 4$ are expected to be detected already down to K = 21, if their typical stellar mass is $\sim 10^{11}$ M$_\odot$ (see Fig. 8). Furthermore, the present, deepest K-band surveys can detect analogous systems with stellar masses as low as $\sim 10^{10}$ M$_\odot$. Thus, present $I_c - K$-selected samples should provide a fair estimate of the co-moving space-density of these systems.

Furthermore, Fig. 8 shows that our models can explain the large fraction of F814W $-$ K$_s$-selected, edge-on disky systems in the Yan & Thompson (2003) sample (with

K$_s$ < 19.5) only if they have stellar masses larger than $\sim 10^{11}$ M$_\odot$, and, possibly, if their characteristic star-formation time scales are as small as 2–3 Gyr (especially for objects at $z \sim 1$).

Finally, edge-on, dusty star-forming disks at $1 \lesssim z \lesssim 2$ with R$_c$ $-$ K > 5.3 are expected to be extremely rare (see Fig. 4 and 5), independent of their mass (not shown). Thus, R$_c$ $-$ K-selected samples are not expected to contain a significant fraction of dusty, star-forming, bulge-less disk galaxies at $1 \lesssim z \lesssim 2$. This is consistent with the recent observational results of Sawicki et al. (2005).

3.2.4 On the star-formation history of the models and the presence of a bulge in real high-z red galaxies

To reproduce the colours/SEDs of continuously star-forming galaxies at high z, other authors (e.g. Förster Schreiber et al. 2004) assume a constant SFR. The $SFR(t)$ of Eq. 1 leads to a constant SFR when $\tau_\star$ tends to infinity. From the previous results we conclude that synthetic, dusty star-forming disks with constant SFR would not meet the colour-selection criteria for high-z red galaxies, whatever the redshift of the model and the attenuation function. The application of Eq. 2 worsens the problem, since it implies younger luminosity-weighted ages, hence bluer observed colours. In conclusion the phase of maximum star-formation activity must be possibly as short as 1 Gyr and must take place at early times. In this case, disks possibly undergo a central gas+stars instability that leads to the formation of a bulge within the same time scale however (see Immeli et al. 2004).

As often discussed in the literature, an alternative explanation for the red colours of real, star-forming disk galaxies at high z is that they are not pure disks, but do contain a bulge. Besides usually containing older stellar populations, a bulge suffers from a larger dust attenuation at rest-frame optical/near-IR wavelengths than a disk, for intermediate/low inclinations. The latter property is a consequence of the difference in dust/stars configuration for the two components (see Ferrara et at. 1999; Tuffs et al. 2004; Pierini et al. 2004b). However before relying on this solution, one has possibly to check the morphology. For instance, only a small fraction of the 24 F814W $-$ K$_s$-selected objects of the Yan et al. (2004) sample seems to be bulge-dominated. On the other hand, of the 24 R $-$ K$_s$-selected objects with K$_s$ < 19 visually classified in both the R and K$_s$ images simultaneously by Sawicki et al. (2005), eleven show clear evidence for the presence of disks, and 10 of the latter eleven[7] exhibit a bulge. Finally, there is an indirect evidence for the presence of a bulge in only 4 distant red galaxies at $z \gtrsim 2$ (photometric, Rubin et al. 2004; Toft et al. 2005).

3.2.5 Geometrically-thin dust lanes at high redshift

When the youngest stars are assumed to be the most embedded in geometrically-thin lanes with e.g. MW-type dust (models A1 through B2), edge-on disk models can exhibit both $I_c - K > 4$ and $J - K > 2.3$ for $2 \times \tau_V \gtrsim 2$ and $2 \lesssim z \lesssim 3.2$, or even R$_c$ $-$ K > 5.3 for $2 \times \tau_V \gtrsim 8$ and

---

[7] The only disk system classified as bulge-less shows signs of interaction.

$1 \lesssim z \lesssim 3.2$ (see Fig. 4). On the other hand, models B4, B5, B7, and B8 can exhibit $I_c - K > 4$ colours only for $1 \lesssim z < 2$, whatever τ_V, and, eventually, $R_c - K > 5.3$ colours only for $2 \times \tau_V > 10$ and $z \sim 1$ (see Fig. 5 for models B5 and B8). Conversely, models B3 and B6 never meet either the $I_c - K > 4$ or the $R_c - K > 5.3$ colour-selection criterion (not shown), though they also reproduce geometrically-thin dust lanes.

Hence, the existence of edge-on, star-forming, bulge-less disk galaxies with $I_c - K > 4$ and $J - K > 2.3$ at $2 < z \lesssim 3.2$ implies that the youngest stars are the most embedded in geometrically-thin dust lanes.

In the local Universe, disk galaxies with geometrically-thin dust lanes seem to have rotational velocities higher than ~ 120 km s^{-1} (Dalcanton et al. 2004). Conversely, nearby disk galaxies with lower rotational velocities exhibit a dust/stars configuration where the dust-to-stars scale-height ratio is close to 1, i.e. as for the S01_ME10 and S01_SE10 dust/stars configurations of Ferrara et al. (1999). Furthermore, Dalcanton et al. (2004) conclude that narrower dust lanes are due to lower characteristic turbulent velocities, as an effect of gravitational instabilities setting in a gas+stars disk. As a consequence, the disk is prone to fragmentation and gravitational collapse along spiral arms.

If these results apply to high-z disk-like galaxies with $I_c - K > 4$ and $J - K > 2.3$, these objects can be expected to experience a relatively efficient, rapid star-formation activity.

3.2.6 On the near-IR colours of Lyman break galaxies

Lyman break galaxies (LBGs) at $2 \lesssim z \lesssim 3.4$ exhibit $0.6 < J - K < 3.2$ (Sawicki & Yee 1998). Their optical and near-IR colours are reproduced fairly well by the starburst models of Vijh, Witt, & Gordon (2003), and seem to be due to reddening by SMC-type dust.

However, our models of dusty, continuously star-forming disks with ages of 1.5–2 Gyr at $2 \lesssim z \lesssim 3.2$ exhibit $2 < J - K < 3$, for a wide region of the explored parameter space (cf. Fig. 4 and 5). They exhibit bluer near-IR colours (down to $J - K \sim 1.6$), if their stellar populations have maximum ages of about 0.6 Gyr (see Fig. 7). This suggests that some of the LBGs with the reddest near-IR colours at $2 \lesssim z \lesssim 3.4$ can be dusty star-forming disks with a prolonged star-formation activity (i.e. with intermediate-age/old stellar populations) and not dusty young starbursts.

An accurate determination of the dynamical mass or, in its absence, of the stellar mass for LBGs at $2 \lesssim z \lesssim 3.4$ can tell if the reddest ones are relatively low-mass starburst systems or massive systems still in the making. An alternative discriminating tool is mid-IR (observed frame) spectroscopy, since the rest-frame visual–near-IR SED of an intermediate-age SSP is characterized by molecular absorption bands originated in the atmospheres of TP-AGB stars (Maraston 2005 and references therein).

3.2.7 On the near-IR colours of submm-sources

Sub-mm galaxies (SMGs, or " SCUBA sources") with confirmed counterparts (based on accurate positions from radio, CO, and/or millimeter continuum interferometric observations) exhibit a median $J - K = 2.6 \pm 0.6$ (Frayer et al. 2004). In particular, the near-IR-bright (i.e. $K < 19$) SMGs exhibit $J - K \simeq 2$, while the near-IR-faint SMGs tend to have $J - K > 3$. Sub-mm sources lie at $2 \lesssim z \lesssim 3$ (Chapman et al. 2003a).

The unresolved, brightest sub-mm sources are held to be systems experiencing a strong tidal interaction/merging (Chapman et al. 2003b; Frayer et al. 2004). However, the SMG investigated by Greve, Ivison, & Papadopoulos (2003) seems to be a very large (several tens of kiloparsecs) system where the dust distribution is more extended than the stellar one, maybe owing to the presence of strong galactic winds. This dust/stars configuration is reminiscent of the Ferrara et al. (1999) configuration S01_ME25 (or S01_SE25) that is included in models B5 (or B8, see Fig. 5). This analogy is intriguing. In fact, Kaviani, Haehnelt, & Kauffmann (2003) show that models of SCUBA sources in which the bulk of the sub-mm emission comes from extended, cold (T ~ 20–25 K) dust in objects with SFRs of 50–100 $M_\odot$ yr^{-1} reproduce the sub-mm counts.

Therefore, it is important to realize that, according to our models, DRdGs may have near-IR colours as red as those of some SMGs, without being necessarily much dustier than the Milky Way.

However, none of our models achieves the reddest near-IR colours observed so far ($J - K \gtrsim 3$–4, Maihara et al. 2001). At least the reddest among these hyper extremely red objects are probably primordial elliptical galaxies reddened by dust and still in the starburst phase of their formation at $z \sim 3$ and, thus, the counterparts of the brightest sub-mm sources, as suggested by Totani et al. (2001).

3.2.8 On the use of single-colour selection criteria

Figures 4 and 5 show that the overlap between $R_c - K$-selected, $I_c - K$-selected, and $J - K$-selected sub-samples of synthetic, dusty star-forming disks is poor. $J - K$-selected models lie mostly at $2 \lesssim z \lesssim 3.2$, while $R_c - K$ and $I_c - K$-selected models lie mostly at $1 \lesssim z \lesssim 2$.

The adoption of arbitrary, single-colour selection criteria introduces a bias not only in redshift but also in the intrinsic properties of the selected objects, as intended at least in part (see Yan & Thompson 2003; Pierini et al. 2004a; Daddi et al. 2004; Yan et al. 2004). Theoretically, this bias arises from the combination of the different rest-frame wavelength ranges probed by the individual broad-band filters with the intrinsic properties (stellar populations and dusty ISM) of the high-z systems.

We illustrate these combined effects through the following example based on our models of dusty, continuously star-forming disks at $0.8 \lesssim z \lesssim 3.2$.

Down to a fixed K-magnitude limit, the $R_c - K > 5.3$ colour-selection criterion drops more (edge-on) disk models than the $I_c - K > 4$ colour-selection criterion. For an aging, dusty, star-forming disk at $z = 1$–2, both the R_c and I_c broad-band filters probe the stellar emission in the rest-frame UV/U-band, dominated by OB stars, after attenuation by internal dust. In particular, for $z = 1$ (2), the R_c band maps the rest-frame wavelength range centred at 3235 Å (2157 Å), while the I_c band maps the rest-frame wavelength range centred at 3932 Å (2622 Å). For $z = 2$, the maximum age of the model stellar populations is about 2.8 Gyr, and, at the systematically shorter, rest-frame near-

UV wavelengths probed by the R_c filter with respect to the I_c filter, the increase in stellar emission overcomes the increase in dust attenuation, whatever the dusty disk model. In fact, the difference in attenuation at the two neighboring rest-frame wavelengths probed by the R_c and I_c filters diminishes when either the inclination or the opacity increases (see Ferrara et al. 1999 and Pierini et al. 2004b). This is so even if the extinction law is of MW type, i.e. has a local absorption peak at 2175 Å. As a result, an aging, dusty star-forming disk at $z \sim 2$ turns out to be "too blue" for the $R_c - K > 5.3$ colour-selection criterion.

On the other hand, for $z = 1$, the age of the model is about 5.3 Gyr and the exact value of the SFR e-folding time becomes important, since now the R_c filter probes also rest-frame near-UV wavelengths, while the I_c filter probes rest-frame wavelengths around the 4000 Å-break. The previous considerations on dust attenuation still apply however. As a result, an aging, dusty, star-forming disk at $z \sim 1$ turns out to be "red enough" for the $I_c - K > 4$ colour-selection criterion. This updates the conclusion of Yan et al. (2004) that the $I_c - K$ is very effective in picking up objects with somewhat prolonged star-formation activity (e.g. with $\tau_\star = 1$ Gyr).

4   SUMMARY AND CONCLUSIONS

This study focusses on those objects discovered at high z that exhibit "red" observed-frame optical/near-infrared (IR) colours ($R_c - K > 5.3$, $I_c - K > 4$, or $J - K > 2.3$) and have been morphologically classified as bulge-less disk galaxies (e.g. Yan & Thompson 2003; Labbé et al. 2003). Disks represent the building blocks of all galaxies with a spheroidal component if the hierarchical galaxy-formation theory holds (e.g. Kauffmann 1996). They also represent the ancestors of bulge+disk galaxies at $z = 0$ for the different scenarios of the so-called "secular evolution" of the bulge-to-disk Hubble sequence, that explain the formation of the bulge component via different mechanisms of disk instability (see Combes 2004 for a recent review).

The aim of this paper is to explore under which conditions of dust attenuation and stellar populations, models with exponentially declining star-formation histories (like those of disks in the local Universe) and without a bulge meet the above mentioned colour-selection criteria. These disk models start forming stars at $z_f = 10$ and at redshifts between 3.2 and 0.8 have ages between 1.5–6 Gyr, solar metallicity, and Salpeter IMF. At variance with other stellar population models, the evolutionary synthesis code used here (Maraston 1998, 2005) includes the contribution of the thermally pulsating phase of an intermediate-mass (2–5 $M_\odot$) star along the Asymptotic Giant Branch (i.e. the TP-AGB phase). The TP-AGB stars are fundamental for computing correctly the emission contribution from intermediate-age (between 0.2 and 1–2 Gyr old), simple stellar populations longward of the rest-frame V band.

The properties of dust attenuation are described by Monte Carlo calculations of radiative transfer of the stellar and scattered radiation through different dusty ISM for a doubly exponential disk geometry (Ferrara et al. 1999; Pierini et al. 2004b). The use of different sets of physically-motivated attenuation functions allows us to probe a large

fraction of the dust-attenuation parameter space, that is still largely unconstrained by observations of high-z objects. This parameter space is defined by variables like the astrophysical properties of the mixture of dust grains present in the ISM (synthesized by the extinction function), the total amount of dust (given by the opacity, i.e. $2 \times \tau_V$ here), the structure of the dusty ISM, and the dust/stars configuration. Therefore the present study complement the others in the literature in which the so-called "Calzetti law" (Calzetti et al. 2000) for starbursts is assumed in order to describe dust attenuation in all star-forming systems at high z.

As a first main result, our synthetic, dusty, star-forming disks at $0.8 \lesssim z \lesssim 3.2$ can exhibit red optical/near-IR colours because of reddening by dust, but only if they have been forming stars for more than ~ 1 Gyr. Otherwise, one has to resort to different characteristics of dust attenuation from those of disks in the local Universe, and/or to star-formation time scales much shorter than 3 Gyr, and/or to the existence of an additional bulge component.

Moreover, our disk models barely exhibit $R_c - K > 5.3$ at $1 \lesssim z \lesssim 2$. They do so only when these three conditions are satisfied: the youngest stars are the most embedded in a narrow dust lane; the disk is viewed at $\sim 90°$; $2 \times \tau_V \gtrsim 6$. One has to resort to star-formation time scales as short as 1 Gyr to obtain disk models with $R_c - K > 5.3$ if viewed at intermediate/low inclinations. Such extremely short star-formation time scales might lead to an early gas+stars disk instability, and, thus, to the formation of a central bulge component (Immeli et al. 2004). Hence, $R_c - K$-selected galaxies observed at $1 \lesssim z \lesssim 2$ are probably either starbursts (Pozzetti & Mannucci 2000) or systems with a bulge, whether they are still forming stars or not. This conclusion is consistent with observational results (e.g. Cimatti et al. 2002; Wilson et al. 2004; Saracco et al. 2005; Severgnini et al. 2005; Sawicki et al. 2005). It is also consistent with the finding that X-ray-selected AGN can exhibit $R_c - K > 5.3$ (Szokoly et al. 2004; Mignoli et al. 2004), if the link beetwen super massive black holes and bulges found in the local Universe holds at high z (Page et al. 2004).

On the other hand, models at $1 \lesssim z \lesssim 2$ can exhibit $I_c - K > 4$ for an inclination close to $90°$, even for very small values of the opacity (i.e. for $2 \times \tau_V > 0.5$). This result holds for a wide range in dust/stars configuration. It can explain the existence of a large fraction (30 per cent) of edge-on (i.e. seen at an inclination close to $90°$), bulge-less disk galaxies with $K_s < 19.5$ and $F814W - K_s > 4$ (Yan & Thompson 2003), some of them at $z \sim 1$ (spectroscopic, see Yan et al. 2004). These results imply that $F814W - K_s$-selected disk galaxies not seen edge on at $1 \lesssim z \lesssim 2$ do have a bulge. Therefore, we can explain why the large majority of the 24 bright, $F814W - K_s$-selected disk galaxies found by Yan et al. (2004) at $0.9 < z < 1.5$ has absorption features from old stars, and why half of the systems with absorption lines experience recent star-formation activity, whatever their morphological classification.

$I_c - K$-selected edge-on models at $1 \lesssim z \lesssim 2$ need to be more massive than $\sim 10^{10}$ $M_\odot$ to be brighter than the limiting magnitude of present K-band surveys (i.e. K = 22.5). In particular, $I_c - K$-selected models at $z \sim 1$ are brighter than $K_s = 19.5$ if they have stellar masses in excess of $\sim 10^{11}$ $M_\odot$ and opacities larger than ~ 2. Therefore, our results point to the existence of massive, star-forming disk-like galaxies at

high z. This is consistent with observational results (Labbé et al. 2003; Stockton et al. 2004; Conselice et al. 2004). Large disk systems may be rare at $z > 1$ (see e.g. Papovich et al. 2005), but their existence, due to an early, rapid evolution, may explain why the size distribution of disk galaxies at $0.25 < z < 1.25$ is consistent with that of disk galaxies in the local Universe, and does not show any significant evolution within this redshift range (Ravindranath et al. 2004).

Furthermore, our models indicate that the edge-on, extremely red (i.e. with $I_c - K > 4$ or $F814W - K_s > 4$), disk-like galaxies at $1 \lesssim z \lesssim 2$ represent just a small fraction of those disks that are at least 1 Gyr-old at look-back times of 7.7–10.2 Gyr. Disks of similar ages at the same redhifts but not seen edge on are expected to have bluer optical/near-IR colours, and, thus, elude the observers' interest.

The previous results are consistent with the finding that the number of $R_c - K$-selected objects is less than the number of $I_c - K$-selected objects out of the same sample of observed high-z galaxies (e.g. Smail et al. 2002). This deficit is due to the coupling of the different rest-frame wavelength ranges covered by the R_c and I_c broad-band filters with the properties of the different, observed stellar systems, in terms of stellar populations (Yan & Thompson 2002; Yan et al. 2004) and of dust attenuation (this study; Pierini et al. 2004a). In general, we confirm that the $I_c - K > 4$ colour-selection criterion picks up objects with evolved stellar populations (e.g. Yan et al. 2004; McCarthy et al. 2004). This does not imply the absence of on-going star formation however.

Synthetic, dusty, continuously star-forming disks at $2 \lesssim z \lesssim 3.2$ can exhibit $J - K > 2.3$ without being necessarily dustier than nearby disk galaxies (with $0.5 \lesssim 2 \times \tau_V \lesssim 2$, Kuchinski et al. 1998). The use of the new stellar populations evolutionary synthesis models including the TP-AGB phase (Maraston 2005) allows to produce disks older than 1 Gyr at $2 \lesssim z \lesssim 3.2$ with $J - K > 2.3$, for a wide range in inclination, dust/stars configuration, and properties of the dusty ISM. Otherwise, one has to resort to values of $\tau_\star$ less than 3 Gyr and/or to introduce a bulge component, or to consider starburst models (e.g. Vijh et al. 2003).

In general, modeling the SED of a high-z galaxy without including the TP-AGB phase and, in addition, with the Calzetti law (e.g. as in the work of Förster Schreiber et al. 2004) may bias the best-fit solution towards older ages and/or higher values of the attenuation (e.g. at the rest-frame V band) and/or larger masses. For instance, our $J - K$-selected models at $z \sim 2.6$ have a minimum rest-frame V-band attenuation of only 0.2 mag (for $i = 70°$) and need to be more massive than $\sim 10^{10} \, M_\odot$ (stellar mass) to be brighter than $K = 22.5$.

Finally, we note that the winds of TP-AGB stars are fundamental contributors to the abundance of Policyclic Aromatic Hydrocarbons (PAH) in the dusty ISM (Gillett, Forrest & Merrill 1973). Thus, disk-like galaxies with $J - K > 2.3$ at $z > 2$ (cf. Labbé et al. 2003; Stockton et al. 2004) may represent dusty objects where the stellar winds of TP-AGB stars appear as a new site for dust formation in addition to the ejecta of Type II supernovae and/or of pair instability supernovae (Todini & Ferrara 2001; Morgan & Edmunds 2003; Nozawa et al. 2003; Hirashita et al. 2005).

REFERENCES

Abraham R. G., Merrifield M. R., 2000, AJ, 120, 2835
Aguirre A., 1999, ApJ, 525, 583
Barnes J. E., Hernquist L., 1992, ARA&A, 30, 705
Bell E. F., 2002, ApJ, 577, 150
Bessel M. S., Brett J. M., 1988, PASP, 100, 1134
Bianchi S., 2004, in Witt A. N., Clayton G. C., Draine B. T., eds, Astrophysics of Dust. ASP, San Francisco, p. 771
Bianchi S., Ferrara A., 2005, MNRAS, 358, 379
Bouwens R. J., Illingworth G. D., Blakeslee J. P., Broadhurst T. J., Franx M., 2004, ApJ, 611, L1
Bruzual A. G., Charlot S., 2003, MNRAS, 344, 1000
Calzetti D., 2001, PASP, 113, 1449
Calzetti D., Kinney A. L., Storchi-Bergmann T., 1994, ApJ, 429, 582
Calzetti D., Armus L., Bohlin R. C., Kinney A. L., Koornneef J., Storchi-Bergmann T., 2000, ApJ, 533, 682
Chapman S. C., Blain A. W., Ivison R. J., Smail I. R., 2003a, Nat, 422, 695
Chapman S. C., Windhorst R., Odewahn S., Yan H., Conselice C., 2003b, ApJ, 599, 92
Charlot S., Fall S. M., 1991, ApJ, 378, 471
Ciardi B., Madau P., 2003, ApJ, 596, 1
Cimatti A., et al., 2002, A&A, 381, L68
Cimatti A., et al., 2003, A&A, 412, L1
Combes F., 2004, astro-ph/0406306
Conselice C. J., et al., 2004, ApJ, 600, L139
Cousins A. W. J., 1978, MNASAA, 37, 8
Daddi E., Cimatti A., Renzini A., Fontana A., Mignoli M., Pozzetti L., Tozzi P., Zamorani G., 2004, ApJ, 617, 746
Dalcanton J. J., Yoachim P., Bernstein R. A., 2004, ApJ, 608, 189
de Bernardis P., et al., 2000, Nat, 404, 955
Dehnen W., Binney J., 1998, MNRAS, 294, 429
Dessauges-Zavadsky M., Calura F., Prochaska J. X., D'Odorico S., Matteucci F., 2004, A&A, 416, 79
Fall S. M., Efstathiou G., 1980, MNRAS, 193, 189
Ferguson H. C., et al., 2004, ApJ, 600, L107
Ferrara A., Bianchi S., Cimatti A., Giovanardi C., 1999, ApJS, 123, 437
Förster Schreiber N. M., et al., 2004, ApJ, 616, 40
Franx M., et al., 2003, ApJ, 587, L79
Frayer T. D., Reddy N. A., Armus L., Blain A. W., Scoville N. Z., Smail I., 2004, ApJ, 127, 728
Gilbank D. G., Smail I., Ivison R. J., Packham C., 2003, MNRAS, 346, 1125
Gillett F. C., Forrest W. J., Merrill K. M., 1973, ApJ, 183, 87
Goldader J. D., Meurer G., Heckman T. M., Seibert M., Sanders D. B., Calzetti D., Steidel C. C., 2002, ApJ, 568, 651
Gordon K. D., Calzetti D., Witt A. N., 1997, ApJ, 487, 625
Gordon K. D., Misselt K. A., Witt A. N., Clayton G. C., 2001, ApJ, 551, 277
Gordon K. D., Clayton G. C., Misselt K. A., Landolt A. U., Wolff M. J., 2003, ApJ, 594, 279

Gordon K. D. et al., 2004, ApJS, 154, 215

Greve T. R., Ivison R. J., Papadopoulos P. P., 2003, ApJ, 599, 839

Haardt F., Madau P., 1996, ApJ, 461, 20

Hernquist L., Springel V., 2003, MNRAS, 341, 1253

Hirashita H., Nozawa T., Kozasa T., Ishii T. T., Takeuchi T. T., 2005, MNRAS, 357, 1077

Immeli A., Samland M., Gerhard O., Westera P., 2004, A&A, 413, 547

Inoue A. K., Kamaya H., 2004, MNRAS, 350, 729

Kajisawa M., Yamada T., 2001, PASJ, 53, 833

Kauffmann G., 1996, MNRAS, 281, 487

Kaviani A., Haehnelt M. G., Kauffmann G., 2003, MNRAS, 340, 739

Keel W. C., White R. E., 2001, AJ, 122, 1369

Kong X., Charlot S., Brinchmann J., Fall S. M., 2004, MNRAS, 349, 769

Kuchinski L. E., Terndrup D. M., Gordon K. D., Witt A. N., 1998, AJ, 115, 1438

Labbé I., et al., 2003, ApJ, 591, L95

Madau P., 1995, ApJ, 441, 18

Maihara T., et al., 2001, PASJ, 53, 25

Mao S., Mo H. J., White S. D. M., 1998, MNRAS, 297, L71

Maraston C., 1998, MNRAS, 300, 872

Maraston C., 2005, MNRAS, in press (astro-ph/0410207)

McCarthy P. J., 2004, ARA&A, 42, 477

McCarthy P. J., et al., 2004, ApJ, 614, L9

Mignoli M., et al., 2004, A&A, 418, 827

Mo H. J., Mao S., White S. D. M., 1998, MNRAS, 295, 319

Mollá M., Ferrini F., & Díaz A. I., 1997, ApJ, 475, 519

Mollá M., Ferrini F., Gozzi G., 2000, MNRAS, 316, 345

Morgan H. L., Edmunds M. G., 2003, MNRAS, 343, 427

Moustakas L. A., et al., 2004, ApJ, 600, L131

Nozawa T., Kozasa T., Umeda H., Maeda K., Nomoto K., 2003, ApJ, 598, 785

Page M. J., Stevens J. A., Ivison R. J., Carrera F. J., 2004, ApJ, 611, L85

Papovich C., Dickinson M., Giavalisco M., Conselice C. J., Ferguson H. C., 2005, astro-ph/0501088

Persson S. E., Aaronson M., Cohen J. G., Frogel J. A., Matthews K., 1983, ApJ, 266, 105

Pierini D., Maraston C., Bender R., Witt A. N., 2004a, MNRAS, 347, 1

Pierini D., Gordon K. D., Witt A. N., Madsen G. J., 2004b, ApJ, 617, 1022

Pozzetti L., Mannucci F., 2000, MNRAS, 317, L17

Ravindranath S. et al., 2004, ApJ, 604, L9

Renzini A., 2004, astro-ph/0410295

Rubin K. H. R., van Dokkum P. G., Coppi P., Johnson O., Förster Schreiber N. M., Franx M., van der Werf P., 2004, ApJ, 613, L5

Salpeter E., 1955, ApJ, 121, 161

Saracco P., et al., 2005, MNRAS, 357, L40

Sawicki M., Yee H. K. C., 1998, AJ, 115, 1329

Sawicki M., Stevenson M., Barrientos L. F., Gladman B., Mallén-Ornelas G., van den Bergh S., 2005, astro-ph/0503523

Schneider R., Ferrara A., Natarajan P., Omukai K., 2002, ApJ, 571, 30

Severgnini P., et al., 2005, A&A, 431, 87

Shapley A. E., Erb D. K., Pettini M., Steidel C. C., Adelberger K. L., 2004, ApJ, 607, 226

Silva L., Granato G. L., Bressan A., Danese L., 1998, ApJ, 509, 103

Smail I., Owen F. N., Morrison G. E., Keel W.C., Ivison R. J., Ledlow M. J., 2002, ApJ, 581, 844

Spergel D. N., et al., 2003, ApJS, 148, 175

Stevens J. A., Page M. J., Ivison R. J., Smail I., Lehmann I., Hasinger G., Szokoly G., 2003, MNRAS, 342, 249

Stockton A., Canalizo G., & Maihara T., 2004, ApJ, 605, 37

Szokoly G. P., et al., 2004, ApJS, 155, 271

Tinsley B. M., 1980, Fund. Cos. Phys., 11, 1

Todini P., Ferrara A., 2001, MNRAS, 325, 726

Toft S., van Dokkum P. G., Franx M., Thompson R. I., Illingworth G. D., Bouwens R. J., Kriek M., 2005, ApJ, 624, L9

Totani T., Yoshii Y., Iwamuro F., Maihara T., Motohara K., 2001, ApJ, 558, L87

Tuffs R. J., Popescu C. C., Völk H. J., Kylafis N. D., Dopita M. A., 2004, A&A, 419, 821

Väisänen P., Johansson P. H., 2004, A&A, 421, 821

van Dokkum P. G., et al., 2004, ApJ, 611, 703

Vijh U. P., Witt A. N., Gordon K. D., 2003, ApJ, 587, 533

White R. E., Keel W. C., Conselice C. J., 2000, ApJ, 542, 761

White S. D. M., Rees M. J., 1978, MNRAS, 183, 341

White S. D. M., Frenk C. S., 1991, ApJ, 379, 52

Whittet D. C. B., 2003, Dust in the galactic environment, 2nd edn. Institute of Physics, Bristol

Wilson G., et al., 2004, ApJS, 154, 107

Witt A. N., Gordon K. D., 1996, ApJ, 463, 681

Witt A. N., Gordon K. D., 2000, ApJ, 528, 799

Yan L., Thompson D., 2003, ApJ, 586, 765

Yan L., Thompson D., Soifer B. T., 2004, AJ, 127, 1274